Molecular and Cellular Neuroscience

Ginkgolic Acid Promotes Autophagy-Dependent Clearance of Intracellular Alpha-Synuclein Aggregates

Shamini Vijayakumaran[1], Yasuko Nakamura[2], Jeremy M. Henley[2] and Dean L. Pountney[1*]

School of Medical Science, Griffith University, Gold Coast, Queensland 4222, Australia.

School of Biochemistry, University of Bristol, Bristol BS8 1TD, UK.

Running title: Ginkgolic acid clears alpha-synuclein aggregates

*Corresponding author: Dean L. Pountney
School of Medical Science,
Griffith University,
Gold Coast, Queensland 4222,
Australia

Tel: +61 7 5552 7273
Fax: +61 7 5552 8908
Email: d.pountney@griffith.edu.au

Abstract:

The accumulation of intracytoplasmic inclusion bodies (Lewy bodies) composed of aggregates of the alpha-synuclein (α-syn) protein is the principal pathological characteristic of Parkinson's disease (PD) and may lead to degeneration of dopaminergic neurons. To date there is no medication that can promote the efficient clearance of these pathological aggregates. In this study, the effect on α-syn aggregate clearance of ginkgolic acid (GA), a natural compound extracted from Ginkgo biloba leaves that inhibits SUMOylation amongst other pathways, was assessed in SH-SY5Y neuroblastoma cells and rat primary cortical neurons. Depolarization of SH-SY5Y neuroblastoma cells and rat primary cortical neurons with KCl was used to induce α-syn aggregate formation. Cells pre-treated with either GA or the related compound, anacardic acid, revealed a significant decrease in intracytoplasmic aggregates immunopositive for α-syn and SUMO-1. An increased frequency of autophagosomes was also detected with both compounds. GA post-treatment 24 hr after depolarization also significantly diminished α-syn aggregate bearing cells, indicating the clearance of pre-formed aggregates. Autophagy inhibitors blocked GA-dependent clearance of α-syn aggregates, but not increased autophagosome frequency. Western analysis revealed that the reduction in α-syn aggregate frequency obtained with GA pre-treatment was not accompanied by a significant change in the abundance of SUMO conjugates. The current findings show that GA can promote autophagy-dependent clearance of α-syn aggregates and may have potential in disease modifying therapy.

Keywords: Parkinson's disease, ginkgolic acid, SUMO, autophagy, alpha-synuclein.

Introduction

Parkinson's disease (PD) is a multi-system proteinopathy reflecting the progressive loss of dopaminergic nigrostriatal neurons causing a variety of motor deficits, including resting tremor, muscular rigidity, bradykinesia and postural instability, and non-motor alterations, such as hypsomia, autonomic and other dysfunctions (Breydo et al., 2012; Eckermann, 2013; Jellinger, 2014). The neuropathological hallmark of PD is the widespread occurrence of intracellular inclusion bodies (Lewy bodies) and neuritic deposits (Lewy neurites) of phosphorylated α-synuclein (α-syn). Although the formation of Lewy bodies is considered a protective cell response, Lewy body maturation eventually becomes toxic triggering neuronal death. The pathological accumulation of intracellular α-syn aggregates is also linked to a variety of other α-synucleopathies, including multiple system atrophy (MSA) and dementia with Lewy bodies (DLB)(Breydo et al., 2012; Radford et al., 2014; Vijayakumaran et al., 2015). Oxidative / nitrosative stress, post-translational modifications, proteolytic stress and calcium dyshomeostasis are some major factors leading to the formation of cytotoxic α-syn species and neuronal degeneration (Nath et al., 2011; Schmid et al., 2013; Wang et al., 2013). Reversal and prevention of α-syn aggregation may provide cytoprotection in α-synucleopathies and there has been significant recent interest in approaches to promote aggregate clearance (Jackrel and Shorter, 2014; Jackson-Lewis et al., 2012; Kalani, 2014; Valera and Masliah, 2013).

Neuropathological α-syn inclusion bodies and α-syn inclusion bodies formed in cell culture experiments accumulate the small ubiquitin-like modifier-1 (SUMO-1) (Pountney et al., 2005; Sarge and Park-Sarge, 2011; Weetman et al., 2013; Wong et al., 2013). SUMOylation is involved in a variety of different cellular pathways by regulating protein-protein or protein-DNA interactions (Krumova et al., 2011; Vijayakumaran et al., 2015, 2018; Henley et al., 2018). As with ubiquitination, SUMOylation involves E1 (SUMO-activating), E2 (SUMO-specific conjugating, Ubc9) and E3 (SUMO ligase, eg., PIAS3) enzymes (Da Silva-Ferrada et al., 2012; Wilkinson et al., 2010). SUMO-1 has been found to associate with cytoplasmic α-syn inclusion bodies in PD, MSA and DLB and also with intranuclear inclusion bodies such as polyglutamine aggregates in Huntington's disease (HD) (Pountney *et al.*, 2005; Pountney *et al*., 2003; Rott *et al.*, 2017). Recent studies suggest that there may be direct and indirect links between

SUMOylation, neurodegenerative disease pathology and cell responses to misfolding and aggregation (Vijayakumaran *et al.,* 2015; 2018; Rott et al., 2017). Wild-type α-syn and disease-linked mutants have been shown to be SUMO substrates indicating direct modulation of protein solubility, whereas links between SUMOylation and autophagy suggest indirect involvement via the cellular response to protein aggregate accumulation (Da Silva-Ferrada et al., 2012; Janer et al., 2010; Kim et al., 2014; Krumova et al., 2011). Moreover, over-expression of PIAS2, the α-syn SUMO ligase resulted in increased accumulation of intracellular aggregates of PD-linked α-syn mutants (Rott et al., 2017). SUMO-1 was also found to be associated with lysosomes clustered around or embedded in α-syn deposits in pathological specimens and cell culture models, where it is conjugated to Hsp90 (Wong *et al*., 2013).

The removal of aggregating protein including misfolded proteins and defective organelles occurs through two main proteolytic pathways; the ubiquitin-proteasome pathway (UPS) and the autophagy-lysosomal pathway (ALP). Defects in these pathways prevent the clearance of proteins from neuronal and glial cytoplasm, leading to a variety of neurodegenerative disorders. Larger protein aggregates as well as damaged organelles are unable to be degraded by the proteasome and are cleared through macroautophagy. Macroautophagy, a prominent constituent of ALP, is a process that involves the bulk lysosomal degradation of soluble and pathological aggregates and damaged organelles (Tanik et al., 2013; Winslow et al., 2010). Defects in ALP have been demonstrated to cause neurodegeneration in animal models deficient in autophagy-related proteins within neuronal tissues as well as human neurodegenerative lysosomal storage diseases (Futerman and van Meer, 2004; Hara et al., 2006; Inoue et al., 2012; Nixon et al., 2008; Tanik et al., 2013).

GA and the related molecule anacardic acid (AA) have been shown to inhibit SUMOylation by blocking the function of Ubc9 (Fukuda et al., 2009). Previous studies have investigated the outcomes of inhibiting the SUMO-pathway using GA, concluding that SUMOylation has a cytoprotective role in maintaining cellular health (Guo et al., 2015; Tossidou et al., 2014). GA and AA, were investigated to determine the effects on α-syn aggregates. GA was found to promote clearance of pre-formed α-syn aggregates at concentrations that were not cytotoxic and resulted in upregulation of macroautophagy, but that had little effect on SUMO conjugates. The

current study suggests that GA or analogues could be useful therapeutics against Parkinson's disease.

Materials and Methods

Cell culture

SH-SY5Y neuroblastoma cells (ATCC® CRL-2266™) were seeded at 10,000 cells per well in 24-well plates on 10 mm glass coverslips for immunofluorescence confocal imaging and analysis. Cells were incubated for a period of 24 h at 37 °C with 5 % CO_2 in 1 mL DMEM/10 % FBS with 0.04 % Amphotericin B and 1 % Strep/Penicillin prior to treatment to allow cells to adhere. In parallel, cells were seeded and incubated in 6-well plates at 300,000 cells per well for cell lysate preparation, SDS-PAGE and Western blotting.

Embryonic cortical neurons were isolated from E18 Wistar Rattus Norvergicus embryos. Cortical areas were dissected and trypsinised, before being plated on PLL-coated 25 mm glass coverslips. Cells were initially plated in plating medium (Neurobasal media + 10% horse serum, B27 supplement, 2 mM Glutamax, 1× penicillin/streptomycin). After 24 hours, the plating medium was replaced with feeding medium (Neurobasal media, B27 supplement, 1.2 mM Glutamax, 1× penicillin/ streptomycin). Cortical neurons were used at DIV7-14 for treatments.

GA/AA treatments

For immunofluorescence analysis, cells were pre-treated with medium containing 6μM to100 μM GA or AA (Calbiochem, USA) for 1 h. Potassium chloride (50mM) was then added to these pre-treated wells and was incubated for 1 h to induce α-syn aggregates as described previously (Follett et al., 2013; Rcom-H'cheo-Gauthier et al., 2014). Wells were then replenished with fresh medium containing GA or AA only for an additional 24 h or 48 h. SH-SY5Y controls of both KCl-depolarised and non-depolarised cells were performed. For gel electrophoresis and western blotting, the experiment was repeated in 6-well plates pre-treated with medium containing 10μM, 40μM and 80μM of GA for 1 h and subsequently depolarized with 50mM KCl for 1 h.

For post-treatment with GA, cells were depolarized with KCl for 1 h without inhibitor pre-treatment. After 24 h, the medium was removed and replenished with fresh medium containing 10μM, 40μM and 80μM of GA for an additional 24 h. Cell lysates from 6-well plates were prepared for gel electrophoresis and Western blot analysis and immunofluorescence results were obtained from coverslips from 24-well plates. After incubation, post-treatment cell viability was determined by MTT assays.

In parallel experiments, KCl-depolarised SH-SY5Y cells were incubated for 23 hours for the induction of α-syn aggregation and were then treated with medium containing the autophagy inhibitors, chloroquine and bafilomycin A1, at 40nM and 10μM, respectively for 1 hour. The medium was then replaced with medium containing 10μM GA as well as the autophagy inhibitors for an additional 24 hours.

All experiments were performed in triplicate.

Immunofluorescence

Coverslips were washed briefly in DPBS prior to fixation. Neuroblastoma cells were fixed and permeabilized with 3:1 methanol: acetone and blocked with 20% normal horse serum (NHS). Primary neurons were fixed in 3.7% v/v paraformaldehyde, 5 % w/v sucrose, PBS (1 h), then quenched (10 m) in 0.1 M glycine, then permeabilized in 0.1 % w/v Triton X-100, 10 NHS. The following primary antibodies were used for immunostaining: monoclonal mouse anti-α-syn antibody (LB509, Invitrogen, 1:100), polyclonal sheep anti-SUMO-1 antibody (Abcam, ab22738, 1:100), polyclonal rabbit Cathepsin-D antibody (Abcam, ab826-250, 1:200) and polyclonal rabbit anti-LC3 antibody (Abcam, ab128025, 1:200). Alexafluor (AF)-conjugated secondary antibodies (Molecular Probes, Invitrogen) AF488 anti-mouse (A21202), AF568 anti-sheep (A21099) and AF647 anti-rabbit (A31573) were used for immunofluorescence and mounted onto microscope slides using Prolong Gold with DAPI mounting medium (Invitrogen). Slides were stored in the dark at 4°C.

Laser Scanning Confocal Microscopy Image Analysis & Cell Counting

Immuno-labelled slides were imaged using the Olympus Fluoview FV-1000 confocal laser scanning microscope. Negative control secondary antibody only slides were imaged to determine the appropriate microscope settings (laser high voltage, electronic gain and offset) for subsequent image analysis. A 60X oil immersion lens was used for imaging. Imaging of DAPI, Alexa-fluor 488, and Alexa-fluor 568 were performed in a single scan from the first channel whereas Alexa-fluor 647 anti-rabbit was imaged in a single scan from the second channel. The channels were then merged, and the images were exported to be edited using the Olympus FV-1000 viewer software. Representative images are shown.

Cells immunostained for SUMO-1 (red) and cathepsin-D (green), lysosomal marker, were analysed for co-localisation. Quantification was performed by counting lysosomes and classifying them as either SUMO-1 positive (yellow), or SUMO-1 negative (red). SUMO-1 positive lysosomes were calculated for α-syn IB-positive or negative. IB-positive cells were classified as bearing distinct bright α-syn puncta as positive aggregates (≥1μm). LC3-positive autophagosomes were counted manually as distinct bright puncta. For autophagy inhibitor treatments, LC3 puncta were analysed using ImageJ (NIH). Background labelling was excluded (0.2%) and LC3 were counted using the Analyse Particles function. Each coverslip had a standard pattern of 5 regions of interest (ROI) and experiments were performed in triplicate (n=15) with ~40 cells counted per ROI. For post-treated cells, immunostained cells were manually counted as IB-positive, bearing large α-syn-positive aggregates (≥2μm) within each ROI (n=10). Images were de-identified to avoid bias. Results were analysed as the proportion of total cells as DAPI-stained nuclei.

Cell Lysate Preparation

Following drug treatments, whole cell protein extracts were prepared using cell lysis buffer (RIPA Buffer, Sigma, R0278) supplemented with protease inhibitor cocktail (1% v/v PIC, Sigma, P8340) and N-ethylmaleimide (50mM NEM, Sigma, E3876). Cells in each 6-well plate were washed briefly in DPBS, scraped and collected in centrifuge tubes, and centrifuged at 2,000

rpm for 5 min. The supernatant was discarded, and the pellet was lysed in RIPA buffer supplemented with PIC and NEM to obtain cytosolic proteins. Protein quantification was performed using the Thermo Scientific BCA Assay kit as per manufacturer's instructions. Equal amounts of sample proteins were diluted in 2x Laemlli buffer containing 5% β-mercaptoethanol (1:1, Sigma, S3401). Samples were boiled at 100^{o}C for 8 minutes prior to loading into gel.

Gel Preparation and Electrophoresis

Samples were subjected to SDS-PAGE using either 10% (SUMO-1) or 12% (LC3) gel densities (40% Acrylamide/Bis 29:1, Bio-Rad, CA, USA). Subsequently, proteins were transferred onto PVDF membranes (Merck Immobilon-P, 0.45um pore size). Membranes were blocked using solutions of either 5% or 3% skim milk and\or bovine serum albumin (BSA) diluted in Tris-buffered saline (TBS) containing 0.1% Tween-20 (TBS-T) for 1 h. Membranes were briefly washed with TBS-T, then probed with the specific primary antibodies at the recommended dilutions by the manufacturer in TBST-T overnight at 4^{0}C with gentle rocking. Primary antibodies were: rabbit anti-SUMO-1 (Abcam, ab3819, 1:1000), rabbit anti-Hsp90 (Cell Signalling, 4877S, 1:1000), rabbit anti-LC3a/b (Abcam, ab128025, 1:1000) and mouse anti-β-actin (Abcam, ab8226, 1:1000). Membranes were washed three times for 5 min each and re-probed for the appropriate HRP-conjugated secondary antibody (Bio-Rad Goat HRP Conjugates; anti-rabbit # 170-6515, anti-mouse #170-6516) suspended in either 5% skim milk or BSA at 1:3000 under room temperature for 1 h. Membranes were washed (3x 5 minutes) where the proteins of interest were detected using the SuperSignal West Femto chemiluminescent substrate (Pierce) and visualized using the ChemiDoc^{TM}XRS+ System (Bio-Rad). The intensity of each protein bands was analysed using the Bio-Rad Image Lab Software.

Statistical analysis

All data were analyzed using Graphpad Prism. Standard error of the mean for graphs was calculated using $(\frac{\sigma}{\sqrt{n}})$. ANOVA tests were conducted to test for statistical significance.

Results

Ginkgolic acid and anarcadic acid decrease □-syn aggregate frequency

To investigate the influence of ginkgolic acid and the structurally-related compound, anacardic acid, on α-syn aggregates, we utilized a well-established PD cell model. Potassium depolarization (1 h) of SH-SY5Y neuroblastoma cells was used to induce a transient increase in intracellular free calcium, resulting in frequent, small cytoplasmic α-syn puncta after 24 h and large, Lewy body-like perinuclear α-syn inclusions after 48 h, as described previously (Follett et al., 2013; Rcom-H'cheo-Gauthier et al., 2014). Under these conditions, it has been shown previously that cytoplasmic inclusion bodies form that are positive for α-syn, thioflavin T, phosphorylated-α-syn, LAMP1 and p62 (Follet et al., 2016; Rcom-H'cheo-Gauthier et al. 2017). SH-SY5Y cells were pre-treated with AA, GA or sham for 1 h. The cells were subsequently depolarized with 50mM KCl for 1 h to raise intracellular free Ca^{2+} and induce α-syn aggregation, then incubated for a further 24 h with or without SUMO-1 inhibitors. Previous studies have shown that 24 h incubations following 1 h KCl depolarisation of SH-SY5Y cells caused frequent α-syn-positive aggregates enabling the use of this as a model for PD (Follett et al., 2013; Rcom-H'cheo-Gauthier et al., 2014). Frequent α-syn puncta were observed in cells treated with 50mM KCl for 1 h after incubation for a further 24 h (Figure 1A) as in the previous studies, which also showed increased α-syn expression (Rcom-H'cheo-Gauthier et al. 2017). Cell counting showed a significant increase in the proportion of aggregate-bearing cells ($p<0.05$) compared to controls (Figure 1C, 2E). To determine the influence of GA or AA treatments on the proportion of α-syn aggregate-positive cells, SH-SY5Y cells were pre-treated with AA or GA before depolarising cells with 50mM of KCl. Subsequently, these cells were incubated in the presence of AA or GA for 24 h. Immunofluorescence staining showed a decrease in the frequency of α-syn puncta in cells co-treated with AA or GA compared to control depolarised SH-SY5Y (Figure 1B, 1D). Cell counting analysis revealed a significant reduction in the proportion of aggregate-bearing SH-SY5Y cells ($p<0.01$) when treated with AA or GA compared to untreated depolarised cells (Figure 1C, 2E). Previous studies have shown that GA treatment can decrease the steady-state level of α-syn (Rott et al., 2017). However, this is the first demonstration that GA (and AA) can reduce the frequency of wild-type α-syn inclusions.

Previous studies have revealed increased levels of SUMO-1-positive lysosomes in α-syn aggregate-bearing cells in MSA brain tissue sections and cell culture models and SUMO-1 associated with CatD-positive domains in intracytoplasmic α-syn inclusion bodies (Wong et al., 2013). More recently, over-expression of the SUMO ligase, PIAS2, was found to boost cytoplasmic α-syn aggregates, whilst treatment with the SUMOylation inhibitor, GA, reduced steady-state α-syn levels (Rott et al., 2017). Immunofluorescence staining showed an increase in SUMOylated lysosomes (yellow puncta) indicating colocalization of CatD and SUMO-1 clustered in a perinuclear location in response to KCl depolarization (Figure 1F, 1G). This is consistent with previous studies showing SUMO-1-positive lysosomes cluster around protein inclusion bodies (Wong et al., 2013). Cells treated with AA or GA, respectively, showed drastically decreased numbers of lysosomes positive for SUMO-1. Cell counting analysis revealed a significant decrease in the co-localisation of SUMO-1 to lysosomes with AA ($p<0.001$) or GA ($p<0.01$) treatments, respectively, compared to untreated depolarized SH-SY5Y (Supp. 1A).

We also investigated the effect of GA on primary rat neurons subjected to the same KCl-depolarization treatment. Figure 2 A-C shows example images of treatments of 7 DIV primary neurons with 0, 25 or 50 mM KCl for 1 h, followed by incubation for 48 h. Treatment with 25 mM KCl (Figure 3 B) resulted in the redistribution of α-syn from cellular processes, becoming more focused in the cell body, accompanied by focal perinuclear accumulations of α-syn (arrows) and enlarged accumulations of α-syn along some processes (arrowheads). Treatment with 50 mM KCl resulted in an increased frequency of focal α-syn aggregates and further reduction in α-syn in the processes (Figure 2 C). Whilst 7 DIV cultures showed little effect on cell morphology from KCl treatment, neuronal cultures treated with KCl at 14 DIV showed frequent cell swelling and retraction of processes (data not shown). In parallel experiments (Figure 2 D-F), co-treatment with 10 μM GA at 7 DIV resulted in reduced MAP-2 marker, α-syn staining of cell bodies and processes and few focal perinuclear or punctate accumulations in cell processes. Due to the diverse population of neurons present and extensive overlap of the cellular network, it was not possible to quantify the effect on α-syn redistribution.

Ginkgolic acid and anacardic acid have little effect on SUMOylation

Western analysis was used to determine the total levels of protein SUMOylation in parallel experiments. Total band integrals showed a significant increase in SUMO-1 conjugates for depolarised SH-SY5Y compared to non-depolarised SHSY5Y ($p<0.05$) for the 90 KDa band, but no significant change for major bands at 80, 75, 30, 20 or 15 KDa, the latter band being attributed to SUMO-1 monomer. Western analysis of the SUMO-1 90kDa band showed a significant decrease at 40μM ($p<0.05$) or 80μM ($p<0.01$) GA for depolarized cells, but no significant change in the other major bands (Figure 3B). Previous immunocapture and reverse immunocapture studies on isolated lysosomes and purified human pathological α-syn inclusions bodies have revealed SUMO-1 conjugated to Hsp90 (Wong et al. 2013). The expression of Hsp90 was increased in KCl depolarized cells and treatment with 80μM GA resulted in a significant reduction in expression in the KCl depolarized cells (Fig. 3 C & D).

To determine the influence of GA under prolonged treatment, experiments were conducted for a period of 48 h both with and without depolarization. There was a substantial reduction of SUMO-1 bands at 100μM inhibitor in both control and KCl-treated cells (Supp. 1B). This is consistent with previous studies of GA cell culture treatments (Rott *et al*., 2017).

Ginkgolic acid and anacardic acid upregulate macroautophagy

In order to investigate the influence of GA and AA on macroautophagy, we investigated the cellular levels of autophagosomes utilizing the autophagosomal marker, LC3. As illustrated in Figure 4A and 4C, the frequency of LC3-positive puncta was found to be upregulated with 10μM AA or GA treatments in depolarized SH-SY5Y. Cell counting analysis of LC3-positive puncta (mean LC3 puncta per ROI) revealed a significant increase in cellular levels of LC3-positive autophagosomes in depolarized and non-depolarized cells ($p<0.05$) treated with 10μM AA or GA (Figure 4B, 4D).

Western analysis showed increased intensity of the LC3b band at 10kDa, indicating increased macroautophagy, in KCl-depolarized SH-SY5Y cells and non-depolarized cells with increasing concentrations of GA (Figure 4E). Western blot integration revealed a significant increase in the LC3b band in depolarized SH-SY5Y at 40μM ($p<0.05$) and 80μM ($p<0.01$) GA treatments and a significant upregulation of the LC3b band at 80μM ($p<0.01$) GA treatments in non-depolarized SH-SY5Y cells (Figure 4F). We therefore confirmed by both imaging and Western analysis that macroautophagosomes are increased in GA and AA treated cells, especially after KCl depolarization.

In parallel experiments, analysis of LC3-positive puncta in 7 DIV primary rat cortical neurons subjected to treatment with 10μM GA showed increased numbers of LC3-positive autophagosomes (arrowheads) in both the processes and cell bodies of 49 ± 5 in KCl depolarized, 24 ± 4 in non-depolarized compared to 8 ± 2 in untreated (Figure 4G).

Post treatment with GA reduces the frequency of □-syn aggregates

We were interested to determine if GA post treatment could promote the clearance of pre-formed α-syn aggregates. To determine if post-treatment with GA influences the frequency of α-syn aggregates, parallel experiments were conducted where the frequency of α-syn-aggregate positive cells was evaluated using immunofluorescence. Figure 5A illustrates the formation of large Lewy body-like structures staining for α-syn in depolarised SH-SY5Y with a 48 h post-depolarization incubation period with no GA treatment. The larger aggregates observed after 48 hr post-depolarization are consistent with previous studies (Follett et al., 2013). The inclusion bodies formed in KCl-depolarized SH-SY5Y cells have been shown previously to stain positively for LB markers, thioflavin T, phosphorylated-α-syn, LAMP1 and p62 (Follet et al., 2016; Rcom-H'cheo-Gauthier et al. 2017). SUMO-1 puncta were clustered around α-syn aggregates as in previous experiments with 1321N1 cells (Wong et al., 3013). In parallel, SH-SY5Y cells were post treated at 24 h after depolarization with GA at 10μM, 40μM and 80μM concentrations, then incubated for a further 24 h with GA present. The frequency of α-syn-positive aggregates was greatly reduced in GA post-treated cells, indicating clearance of pre-

formed aggregates (Figure 5B). A few large and several small aggregates were observed with 10μM GA post-treatments, a few small aggregates were observed with 40μM GA and almost no aggregates were detected at 80μM GA (Figure 5B). Cell counting analysis of large (≥2μm) α-syn-positive aggregate-bearing SH-SY5Y cells showed a significant decrease in cells bearing α-syn positive IB in depolarised cells when treated with increasing concentrations of GA at 10μM, 40μM and 80μM ($p<0.0001$) (Figure 5C). There were no large aggregates found in non-depolarised SH-SY5Y. At 48 h post depolarization, SH-SY5Y cells showed no significant difference in viability by MTT assay, compared to non-depolarized cells (Figure 5 D). The addition of 10μM GA at 24 h had no effect on viability. However, at 40μM and 80μM GA, there was a significant increase ($p<0.001$) in viability in depolarized, compared to control, with 80μM GA resulting in a 20% reduction in viability in non-depolarized, compared to control (($p<0.05$).

Post treatment with GA has little effect on SUMOylation

In order to evaluate the SUMOylation level in cells post-treated with GA at increasing concentrations, we first allowed potassium depolarized SH-SY5Y cells to incubate for 24h to induce α-syn-positive aggregates within cells and subsequently treated cells with increasing concentrations of 10μM, 40μM and 80μM GA for an additional 24 h (Figure 6A). Figure 6B illustrates the comparison of the SUMO-1 90 KDa band, showing that for 10 μM ($p<0.05$), 40μM ($p<0.05$) and 80μM ($p<0.01$) GA treatments, integration of cellular levels of the 90kDa SUMO-1 band were significantly reduced compared to no SUMO-1 inhibition in depolarized SH-SY5Y cells (Figure 6B). We observed no significant difference in this band at 10 μM GA in the pre-treatment experiments. None of the other major SUMO-1 conjugates was significantly different. Western analysis of Hsp90 similarly revealed a decrease in the depolarized cells at 40μM ($p<0.05$) and 80μM ($p<0.05$) GA treatments (Figure 6C, D).

Post treatment with GA upregulates macroautophagy

Parallel experiments were conducted to evaluate the cellular levels of LC3-positive autophagosomes in cells depolarised with KCl that were subjected to post-treatments with GA at

increasing concentrations. Figure 7A represents images of SH-SY5Y cells stained for LC3 (red). When compared to depolarised cells without GA treatment, depolarised cells subjected to 10μM GA showed a distinct upregulation of LC3-positive puncta (Figure 7A). Western analysis of cell lysates subjected to post GA treatment showed a prominent upregulation of the LC3b band, particularly at 80μM GA, as seen in Figure 7B. Band integration showed that LC3b was significantly upregulated ($p<0.01$) in cells subjected to 80μM GA treatment in depolarized cells (Figure 7C).

GA-mediated clearance of pre-formed intracellular α-syn aggregates is autophagy-dependent

In order to determine if the GA-mediated clearance of α-syn aggregates in KCl-depolarized SH-SY5Y cells is dependent on lysosomal activity, we conducted a series of parallel experiments where cells were first subjected to depolarization with 50 mM KCl, then incubated for 23 hours to form aggregates. Cells were then incubated for 1 hour with either chloroquine or bafilomycin A1, to block autophagy, or vehicle then were treated with 10 μM GA in the presence of the autophagy inhibitors for a further 24 hr. Immunofluorescence analysis revealed that there was no significant difference in the proportion of α-syn aggregate bearing cells in cells that received either of the autophagy inhibitor treatments in addition to GA, compared to KCl only, whereas, the control experiments showed a significant reduction in aggregates with GA treatment in comparison both to no GA ($p<0.001$), or GA plus either chloroquine or bafilomycin A1 ($p<0.05$)(Figure 8 A – F). Conversely, analysis of the frequency of LC3-positive puncta (Figure 8 G - L) showed that combined GA and autophagy inhibitor treatment each resulted in significantly increased LC3-positive autophagosomes per cell compared to non-depolarized or KCl-depolarised ($p<0.001$), with no significant differences between the combined treatments and GA only.

Discussion

The current study incorporated the use of an α-syn aggregation cell model of PD, whereby KCl was used to induce membrane depolarization in SH-SY5Y neuroblastoma cells or rat cortical neurons, leading to formation of frequent microscopically-visible α-syn aggregates over the subsequent 24-48 hrs. GA and AA that both have inhibitory activity towards the ubc9-enzyme in the SUMO pathway were utilized to determine their influence on the accumulation of α-syn aggregates after 24 hr incubations with the inhibitors. GA in particular was found to result in reduced α-syn aggregates and increased macroautophagy markers and was able to promote the clearance of pre-formed α-syn aggregates.

In previous studies, it was determined that SUMO-1 marks a subset of lysosomes that cluster around pathological α-syn inclusion bodies and tau deposits in MSA and progressive supranuclear palsy (PSP) brain tissue, respectively (Wong et al., 2013). Hsp90 has been identified to be associated with SUMO-1 in pathological intra-nuclear inclusion bodies (Pountney et al., 2008) and glial α-syn aggregates (Wong et al., 2013). SUMOylation of Hsp90 has also been shown to modulate the interaction with the Aha1 co-chaperone (Mollapour et al., 2014). Thus, SUMO-1 modification of hsp90 may be linked to the molecular cascade of the autophagy lysosome system when cells respond to an accumulation of aggregates that cause neurodegeneration. SUMOylation was also upregulated in the lesioned hemisphere of a unilateral rotenone lesion model of PD (Weetman et al., 2013). We hypothesized that inhibiting protein SUMOylation using SUMO E1-enzyme (Ubc9) inhibitors to partially inhibit SUMOylation may influence the autophagy lysosome system and affect the turnover of α-syn aggregates in a cellular PD model. However, although GA was confirmed to cause significant inhibition of SUMOylation at 100 μM as established in earlier studies, at the 10μM concentration that effectively promoted α-syn aggregate clearance, there was very little influence on the expression of SUMO-conjugates. Only the 90 KDa SUMO band associated with the occurrence of α-syn aggregates was affected at this concentration of GA. Other mechanisms may therefore come into play to mediate GA-dependent aggregate clearance. For example, GA has been shown to efficiently potentiate glycine-dependent activation of the α1-glycine receptor at a concentration

of 3μM GA (Maleeva et al., 2015). GA has also been shown to inhibit fatty acid synthase and HIV protease, modulate Bcl-2/Bax apoptosis effectors and inhibit various phosphatases, including in the STAT3 signalling pathway, although most of these activities are in the 100 μM or more range.

SUMOylation of lysosomes and SUMO-1 staining of aggregates was increased in response to α-syn aggregation in the SH-SY5Y cell model. We found that GA and AA resulted in reduced frequencies of SUMO-positive perinuclear puncta and SUMO-1-positive lysosomes. GA and AA upregulated LC3-positive autophagosomes and reduced the frequency of intracellular α-syn-positive inclusion bodies in potassium depolarized SH-SY5Y neuroblastoma cells. Similar results were also obtained in 7 DIV primary rat cortical neurons. Similar to the results obtained in previous studies (Wong et al., 2013), SUMO-1 was found to be co-localised with the cathepsin-D (CATD) lysosomal marker in aggregate positive cells. Using low doses of AA or GA (10μM), SUMO-1 colocalization with CatD-positive lysosomes in IB-positive cells were significantly reduced. Western analysis for SUMO-1 showed that GA caused a slight reduction only in the 90 KDa SUMO-1 band, whilst other major SUMO-1 conjugates were unaffected at this low concentration of GA. Whilst 10μM GA had little effect on total SUMO-1 conjugates, there was a four-fold reduction of SUMO-1 associated with lysosomes, suggesting a greater sensitivity of the lysosomal SUMO-conjugates to GA treatment. As SUMO-positive lysosomes have been shown to be associated with α-syn (and polyglutamine) aggregates under a variety of conditions in previous cell culture experiments (Wong et al., 2013), this effect may be associated with the clearance of α-syn aggregates, although we cannot exclude a direct effect on SUMOylation. This low dose of GA also showed no significant cytotoxicity. Whereas, cells subjected to 100μM GA showed 80-90% loss of SUMO-1 conjugates and 80μM GA resulted in 20 % decreased viability in non-depolarized cells, consistent with toxicity. The combination of GA and depolarization increased viability which is difficult to interpret, but may be due to effects on cell signalling.

In our autophagy inhibitor treatment experiments, treatment with chloroquine inhibits autophagic flux by decreasing autophagosome-lysosome fusion (Mauthe et al., 2018). Therefore, increased autophagosome formation stimulated by GA treatment led to increased autophagosome numbers,

but did not result in productive autophagy and subsequent clearance of α-syn aggregates. Similarly, the vesicular ATPase (V-ATPase) inhibitor, bafilomycin A1, disrupts autophagic flux by inhibiting V-ATPase-dependent lysosome acidification and autophagosome-lysosome fusion (Mauzevin and Neufeld, 2015). Our studies therefore suggest that GA-mediated clearance of α-syn aggregates requires active macroautophagy and the fusion of autophagic vesicles with lysosomes.

Reports have suggested that SUMOylation of substrate proteins may have an endogenous neuroprotective response. It has been shown that the overexpression of SUMO increases cell survival under oxygen and glucose deprivation whereby the knockdown of SUMO proved to be deleterious. Conversely, down regulating SUMOylation of proteins in diseases characterised by hyper SUMOylation is also beneficial. (Cimarosti et al., 2012; Datwyler et al., 2011; Guo et al., 2015; Silveirinha et al., 2013; Wilkinson et al., 2010). An *in vitro* study also revealed the neuroprotective role of SUMO in that the SUMOylation of a small portion of α-syn was able to prevent its aggregation (Abeywardana and Pratt, 2015). Consistent with that finding, a cell culture study showed that SUMO-deficient α-syn presented with exacerbated aggregation causing cellular toxicity (Krumova et al., 2011). More recently, the SUMO ligase PIAS2 was found to directly SUMOylate α-syn and overexpression of PIAS2 could increase intracellular aggregates of α-syn PD-linked mutants (Rott *et al.*, 2017). Moreover, GA treatment of HEK293 cells over-expressing α-syn or primary rat neurons reduced the steady-state level of wild-type α-syn (Rott *et al*., 2017).

It has been suggested that SUMOylation of lysosomal Hsp90 may be important for its function in CMA (Vijayakumaran et al., 2015, 2018). Previous studies have evaluated the SUMO-1 labelling of lysosomes in cells treated with proteasome inhibitor, MG132, showing an increase in the 90kDa SUMO-1-positive band that was immunopositive for Hsp90 and identifying via immunocapture the lysosomal SUMO-conjugate of Hsp90 that was also present in purified human pathological α-syn aggregates (Wong et al., 2013). In the current study, the SUMO-1 positive band at 90kDa showed significant decrease at increasing concentrations of GA in depolarized cells. The same SUMO-1-positive 90 KDa band was also increased in the depolarized aggregate bearing cells that were not GA treated. As GA is only applied during the

time that cells are responding to aggregate burden, the selective effects on the 90 KDa band may indicate that there is little influence on the equilibrium levels of other SUMO conjugates over the 24 hr timescale of GA treatment. It has been shown previously that inhibition of Hsp90 induces macroautophagy and reduces the aggregation of α-syn (Chaari et al., 2013; Riedel et al., 2010; Xiong et al., 2015; Vijayakumaran et al., 2015). SUMOylation of Hsp90 has been shown to inhibit the interaction with the Aha1 co-chaperone (Mollapour et al., 2014). Therefore, inhibiting Hsp90 SUMOylation could result in an effective downregulation of Hsp90 activity and consequently an increase in macroautophagy. The current data does not provide a direct link between inhibiting Hsp90 SUMOylation and the increased macroautophagy observed. However, both GA and AA treatments resulted in similar increases in macroautophagy and reduction in SUMO-1 90 KDa conjugates. The SUMO pathway could influence autophagy via multiple factors. Indeed, SUMOylation of Vps34, which forms part of the autophagosome machinery, also has the potential to modulate macroautophagy (Yang et al., 2013). Moreover, Cuervo and co-workers have proposed that synergy between macroautophagy and CMA is crucial in PD (Cuervo and Wong, 2014). Thus, inhibiting the SUMOylation of lysosomal Hsp90, which occurs in response to protein aggregates, may be able to affect the balance between CMA and macroautophagy. Inhibiting Hsp90 activity could also influence autophagosome formation via the mTor signalling pathway. Conversely, promoting clearance of α-syn aggregates would in itself also result in reduced Hsp90 and reduced Hsp90-SUMO-1 conjugate.

We investigated LC3 as a marker of autophagosomes in α-syn aggregate positive and GA and AA treated cells. Western blot analysis showed that LC3b, an indicator of macroautophagic activity, showed no significant changes in cellular levels when comparing aggregate-positive cells to controls in post-treated cells. This was consistent with the results obtained with immunofluorescence staining of cells, where there were no significant changes in levels of LC3-positive puncta. However, when cells were subjected to GA treatments, Western blot analysis showed a significant increase in LC3b. Parallel results were observed in cells immunostained for LC3, showing an increase in LC3-positive puncta in aggregate-bearing cells treated with GA. Furthermore, the observed puncta were much larger than those found in control cells. These results indicate that GA/AA may cause an upregulation of macroautophagy. Previous studies have shown that α-syn is preferentially degraded by CMA, yet aggregation-prone PD-linked α-

syn mutants are not able to be degraded by CMA, binding to the LAMP2A pore and inhibiting lysosomal degradation (Cuervo *et al*., 2004). Thus, promoting macroautophagy may overcome the block to CMA in response to α-syn aggregates, resulting in clearance of α-syn aggregates.

The current study investigated α-syn aggregates in KCl-depolarised cells treated with GA (and AA) to determine if these reagents could affect the frequency of α-syn aggregates. Immunofluorescence of aggregate positive cells compared to those treated with increasing concentrations of GA showed a significant and progressive decrease in α-syn-positive aggregates. Large aggregates (≥2μm) that were observed in aggregate positive cells with no GA treatment resembled the Lewy body IBs observed in neuropathological tissue. However, these large aggregates were greatly diminished when treated with GA, with some small aggregates (<2μm) being present at low GA concentration and an almost total absence of microscopically-visible aggregates at higher GA concentrations.

The upregulation of LC3 puncta observed in depolarised cells treated with GA suggests that cells upregulated the level of autophagosomes. This indicates that cells treated with GA activate macroautophagy thereby mediating α-syn aggregate clearance, that may overcome the block to CMA-mediated α-syn degradation caused by the binding of α-syn aggregates to autophagy components. This was confirmed by experiments that showed that blocking autophagy also blocked aggregate clearance, but did not suppress the GA-mediated increase in frequency of autophagosomes. Moreover, this finding indicates that the activation of macroautophagy by GA may be beneficial in protecting neural cells against toxic stress due to the accumulation of α-syn aggregates. Thus, GA may stimulate α-syn aggregate clearance by upregulating macroautophagy and could represent a new therapeutic target in PD. Further studies will be required to better elucidate the mechanism of GA in promoting autophagy; whether this is dependent on the inhibition of SUMOylation and if Hsp90 plays a role.

Acknowledgments

Financial assistance of Griffith University and University of Bristol is gratefully acknowledged. We thank Mary-Louise Villones and Michael Goulding for assistance.

Figure Legends

Figure 1. Ginkgolic acid and anacardic acid yield reduced □-syn aggregates. (A) Comparison of control SH-SY5Y to 50mM KCl depolarized SH-SY5Y (24 h). Immunofluorescence showed increased α-syn puncta in KCl depolarised SH-SY5Y (green). (Scale bar, 20μm). (B) Immunofluorescence staining comparing depolarized SH-SY5Y to AA treated, depolarized SH-SY5Y. (C) Cell counting analysis of AA treatments of depolarized and non-depolarised SH-SY5Y indicating a significant decrease in α-syn positive aggregates in AA-treated cells. (D) Immunofluorescence staining of depolarized control SH-SY5Y compared to GA treated, depolarized SH-SY5Y. (Scale bar, 10μm). (E) Cell counting analysis of GA treatments of depolarized and non-depolarised SH-SY5Y show a significant decrease in α-syn positive aggregates in SH-SY5Y in GA-treated cells. (F), (G) SUMO-1-immunofluoescence of depolarized SH-SY5Y cells for controls and AA- or GA-treatments (24 h). Arrows indicate yellow puncta and inclusion bodies from co-localised SUMO-1 (red) to lysosomes (Cathepsin D; green). (Scale bar, 20μm). (B)Error bars indicate SEM. * = p, 0.05; ** = p, 0.01; *** = p, 0.001; **** = p, 0.0001.

Figure 2. Rat cortical primary neurons show reduced □-syn aggregates upon ginkgolic acid treatment. (A-C) Representative images of 7 DIV primary neurons treated with 0, 25 mM or 50 mM KCl for 1 h, then incubated for 48 h. (D-F) Representative images of co-treatments with 10μM GA. Red, MAP2. Green, α-syn. Blue, DAPI.

Figure 3. Ginkgolic acid treatment has little effect on SUMO-1 conjugates. (A)Western blot showing SUMO-1 bands of depolarized and non-depolarised SH-SY5Y under increasing concentrations of GA at 10μM, 40μM, 80μM. (B) Western blot analysis of SUMO-1 with GA treatments in depolarized and non-depolarised SH-SY5Yshowing a significant decrease in SUMO-1 band intensity at 40μM and 80μM GA only for the 90 KDa band that increased upon KCl depolarization. (C) Western blot for Hsp90 with different GA treatment concentrations. (D) Western blot analysis showed a significant increase after KCl depolarisation and a significant decrease at 80μM GA in depolarized SH-SY5Y cell lysates. Error bars indicate the SEM. * = p, 0.05; ** = p, 0.01; *** = p, 0.001; **** = p, 0.0001.

Figure 4. Frequency of LC3-positive autophagosomes increases with GA and AA treatment in depolarized and non-depolarised SH-SY5Y. (A), (C) Immunofluorescence (24 h) showing LC3-positive puncta (red) in depolarized SH-SY5Y show significant increases in LC3 puncta upon GA and AA treatments. (Scale bar, 20μm). (B), (D) Cell counting analysis of LC3-positive autophagosome levels with GA and AA in depolarized and non-depolarized SH-SY5Y indicate a significant upregulation of the frequency of LC3-positve autophagosomes. (E) Representative Western blot (48 h) illustrating the LC3a (15kDa) and LC3b (10kDa) bands at increasing concentrations of GA in depolarized and non-depolarized SH-SY5Y, showing increased intensity of the LC3b band at concentrations of GA at 40μM and 80μM. (F) Integration of LC3b in depolarized and non-depolarized SH-SY5Y at increasing concentrations of GA indicate a significant increase in LC3b in non-depolarised SHSY5Y at 40μM and 80μM GA and at 80μM GA in depolarised SH-SY5Y. (G) 7 DIV Rat cortical primary neurons subjected to 10μM GA, with or without KCl depolarization, showing increased LC3-positive autophagosomes (arrowheads). Blue, DAPI. Red, SUMO-1. Lilac, LC3. Green, α-syn. Error bars indicate SEM. * = p, 0.05; ** = p, 0.01; *** = p, 0.001; **** = p, 0.0001.

Figure 5. Reduced frequency of □-syn-positive aggregates in depolarised SH-SY5Y cells subjected to GA post-treatment. (A) Immunofluorescence of SH-SY5Y subjected to KCl-depolarisation and incubation for 48 h where the presence of large and small Lewy-body-like α-syn-positive aggregates in cells was observed in KCl depolarised SH-SY5Y (arrows). (Inset) Co-labelling revealed frequent cytosolic SUMO puncta in α-syn-positive cells (arrowhead) (Scale bar, 10μm). (B) SH-SY5Y subjected to post-treatments of GA at various concentrations indicating large and small α-syn aggregates in SH-SY5Y cells (arrows) where there is a decrease in the frequency of α-syn positive cells at 10μM treatments of GA and only small and less frequent α-syn-positive aggregates in cells subjected to higher concentrations of GA at 40μM and 80μM. (Scale bar, 10μm). (C) Cell counting analysis of the proportion of aggregate-bearing non-depolarised and depolarised SH-SY5Y. There were no large aggregates present in cells of non-depolarised SH-SY5Y. The percentage of aggregate-bearing cells in KCl depolarised SH-SY5Y increased significantly when compared to control. The percentage of aggregate-bearing cells were significantly decreased at 10μM, 40μM and 80μM GA treatments. (D) MTT cell viability assays of SH-SY5Y cells subjected to 1 h depolarization with 50 mM KCl, then 48 h

incubation, treated with increasing concentrations of GA at 24 h post depolarization. Error bars indicate SEM. * = p, 0.05; ** = p, 0.01; *** = p, 0.001; **** = p, 0.0001.

Figure 6. SUMO-1 conjugates in SH-SY5Y cells after post-depolarisation treatment with GA. (A) Western blot illustrating SUMO-1 bands comparing cell lysates subjected to increasing concentrations of GA at 10μM, 40μM and 80μM in depolarised and non-depolarised SH-SY5Y. (B) Integrated SUMO-1-conjugate band intensity at various concentrations of GA in depolarised and non-depolarised SH-SY5Y cell lysates indicating a significant increase in the integrated SUMO-1 bands when treated with KCl. GA treatments at 40μM and 80μM GA show a decrease in the integrated SUMO-1 only for the 90KDa band in depolarised SH-SY5Y. (C) Western blot of Hsp 90 in depolarised and non-depolarised SH-SY5Ycell lysates subjected to increasing concentrations of GA. (D) Integration of the Hsp 90 band shows a significant decrease in the intensity at 40μM and 80μM GA treatments in depolarised SH-SY5Y. Error bars indicate SEM. * = p, 0.05; ** = p, 0.01; *** = p, 0.001; **** = p, 0.0001.

Figure *7*. Increased LC3-positive autophagosomes and LC3b expression in GA post-treated depolarised and non-depolarised SH-SY5Y cells. (A) Immunofluorescence representative images of GA treated depolarised and non-depolarised SH-SY5Y showing LC3-positive autophagosome puncta (red) show upregulation in LC3-positive puncta (red) in non-depolarised and depolarised SH-SY5Y. (Scale bar, 10μm). (B) Western blot illustrating LC3a (15 kDa) and LC3b (10kDa) bands of depolarised and non-depolarised SH-SY5Y cell lysates subjected to various concentrations of GA post-treatment. (C) Western blot analysis comparing LC3b band intensity of depolarised and non-depolarised SH-SY5Y subjected to various post-treatments with GA indicating a significant upregulation of LC3b ratio in cell lysates subjected to 80μM GA. Error bars indicate SEM. * = p, 0.05; ** = p, 0.01; *** = p, 0.001; **** = p, 0.0001.

Figure 8. Autophagy inhibitors block □-syn aggregate clearance in post-GA-treated KCl-depolarized SH-SY5Y cells. (A-F) Bafilomycein A1 or chloroquine pre-treatment (24 hr post-KCL-depolarization) results in no significant differences in aggregate frequency with or without GA treatment. (G-L) Bafilomycin A1 or chloroquine pre-treatment of SH-SY5Y cells has no

significant effect in LC3-positive autophagosome frequency in GA-treated KCl-depolarized cells. Scale bars, 20 μM. Error bars indicate SEM. * = p, 0.05; ** = p, 0.01; *** = p, 0.001; **** = p, 0.0001.

Supplementary Figure 1. (A) Cell counting analysis of SUMO-1 positive lysosomes with AA or GA treatments in non-depolarised and depolarized SH-SY5Y, showing a significant decrease in the percentage of SUMO-1 positive lysosomes is observed in depolarised SH-SY5Y treated with AA or GA. (B) Western blot analysis comparing the integration of SUMO-1 bands in both non-depolarised and depolarized SH-SY5Y with GA treatments (48 h), indicating a significant decrease in the percentage of SUMO-1 integrated bands at 100μM GA.

References

Abeywardana, T., Pratt, M.R., 2015. Extent of Inhibition of α-Synuclein Aggregation in Vitro by SUMOylation Is Conjugation Site-and SUMO Isoform-Selective. Biochemistry 54, 959-961.

Breydo, L., Wu, J.W., Uversky, V.N., 2012. α-Synuclein misfolding and Parkinson's disease. Biochimica et Biophysica Acta (BBA) - Molecular Basis of Disease 1822, 261-285.

Chaari, A., Hoarau-Véchot, J., Ladjimi, M., 2013. Applying chaperones to protein-misfolding disorders: Molecular chaperones against α-synuclein in Parkinson's disease. International Journal of Biological Macromolecules 60, 196-205.

Cimarosti, H., Ashikaga, E., Jaafari, N., Dearden, L., Rubin, P., Wilkinson, K.A., Henley, J.M., 2012. Enhanced SUMOylation and SENP-1 protein levels following oxygen and glucose deprivation in neurones. Journal of cerebral blood flow and metabolism : official journal of the International Society of Cerebral Blood Flow and Metabolism 32, 17-22.

Cuervo AM, Stefanis L, Fredenburg R, Lansbury PT, Sulzer D. 2004. Impaired degradation of mutant alpha-synuclein by chaperone-mediated autophagy. Science. 305, 1292-5.

Cuervo, A.M., Wong, E., 2014. Chaperone-mediated autophagy: roles in disease and aging. Cell Res 24, 92-104.

Da Silva-Ferrada, E., Lopitz-Otsoa, F., Lang, V., #xe9, rie, Rodr, #xed, guez, M.S., Matthiesen, R., 2012. Strategies to Identify Recognition Signals and Targets of SUMOylation. Biochemistry Research International 2012, 16.

Daturpalli, S., Waudby, C.A., Meehan, S., Jackson, S.E., 2013. Hsp90 Inhibits α-Synuclein Aggregation by Interacting with Soluble Oligomers. Journal of Molecular Biology 425, 4614-4628.

Datwyler, A.L., Lattig-Tunnemann, G., Yang, W., Paschen, W., Lee, S.L., Dirnagl, U., Endres, M., Harms, C., 2011. SUMO2/3 conjugation is an endogenous neuroprotective mechanism. Journal of cerebral blood flow and metabolism : official journal of the International Society of Cerebral Blood Flow and Metabolism 31, 2152-2159.

Eckermann, K., 2013. SUMO and Parkinson's disease. Neuromolecular Med 15, 737-759.

Follett, J., Darlow, B., Wong, M., Goodwin, J., Pountney, D., 2013. Potassium Depolarization and Raised Calcium Induces α-Synuclein Aggregates. Neurotox Res 23, 378-392.

Fukuda, I., Ito, A., Hirai, G., Nishimura, S., Kawasaki, H., Saitoh, H., Kimura, K., Sodeoka, M., Yoshida, M., 2009. Ginkgolic acid inhibits protein SUMOylation by blocking formation of the E1-SUMO intermediate. Chem Biol 16, 133-140.

Futerman, A.H., van Meer, G., 2004. The cell biology of lysosomal storage disorders. Nat Rev Mol Cell Biol 5, 554-565.

Guo, C., Wei, Q., Su, Y., Dong, Z., 2015. SUMOylation occurs in acute kidney injury and plays a cytoprotective role. Biochim Biophys Acta 1852, 482-489.

Hara, T., Nakamura, K., Matsui, M., Yamamoto, A., Nakahara, Y., Suzuki-Migishima, R., Yokoyama, M., Mishima, K., Saito, I., Okano, H., Mizushima, N., 2006. Suppression of basal autophagy in neural cells causes neurodegenerative disease in mice. Nature 441, 885-889.

Henley JM, Carmichael RE, Wilkinson KA (2018) Extranuclear SUMOylation in Neurons. *Trends Neurosci.* **41**, 198-210.

Inoue, K., Rispoli, J., Kaphzan, H., Klann, E., Chen, E.I., Kim, J., Komatsu, M., Abeliovich, A., 2012. Macroautophagy deficiency mediates age-dependent neurodegeneration through a phospho-tau pathway. Molecular Neurodegeneration 7, 48.

Jackrel, M.E., Shorter, J., 2014. Reversing deleterious protein aggregation with re-engineered protein disaggregases. Cell Cycle 13, 1379-1383.

Jackson-Lewis, V., Blesa, J., Przedborski, S., 2012. Animal models of Parkinson's disease. Parkinsonism & Related Disorders 18, Supplement 1, S183-S185.

Janer, A., Werner, A., Takahashi-Fujigasaki, J., Daret, A., Fujigasaki, H., Takada, K., Duyckaerts, C., Brice, A., Dejean, A., Sittler, A., 2010. SUMOylation attenuates the aggregation propensity and cellular toxicity of the polyglutamine expanded ataxin-7. Hum Mol Genet 19, 181-195.

Jellinger, K.A., 2014. The pathomechanisms underlying Parkinson's disease. Expert review of neurotherapeutics 14, 199-215.

Jiang, T.-F., Zhang, Y.-J., Zhou, H.-Y., Wang, H.-M., Tian, L.-P., Liu, J., Ding, J.-Q., Chen, S.-D., 2013. Curcumin Ameliorates the Neurodegenerative Pathology in A53T α-synuclein Cell Model of Parkinson’s Disease Through the Downregulation of mTOR/p70S6K Signaling and the Recovery of Macroautophagy. Journal of Neuroimmune Pharmacology 8, 356-369.

Kalani, A., 2014. Exosomes: Mediators of Neurodegeneration, Neuroprotection and Therapeutics. Molecular neurobiology 49, 590-600.

Kim, W.S., Kågedal, K., Halliday, G.M., 2014. Alpha-synuclein biology in Lewy body diseases. Alzheimer's research & therapy 6, 73.

Krumova, P., Meulmeester, E., Garrido, M., Tirard, M., Hsiao, H.-H., Bossis, G., Urlaub, H., Zweckstetter, M., Kügler, S., Melchior, F., Bähr, M., Weishaupt, J.H., 2011. Sumoylation inhibits α-synuclein aggregation and toxicity. The Journal of Cell Biology 194, 49-60.

Maleeva G, Buldakova S, Bregestovski P. 2015. Selective potentiation of alpha 1 glycine receptors by ginkgolic acid. Front Mol Neurosci. 8:64.

Mauthe M, Orhon I, Rocchi C, Zhou X, Luhr M, Hijlkema KJ, Coppes RP, Engedal N, Mari M, Reggiori F., 2018. Chloroquine inhibits autophagic flux by decreasing autophagosome-lysosome fusion. Autophagy 14, 1435-1455.

Mauvezin C, Neufeld TP., 2015. Bafilomycin A1 disrupts autophagic flux by inhibiting both V-ATPase-dependent acidification and Ca-P60A/SERCA-dependent autophagosome-lysosome fusion. Autophagy 11, 1437-8.

Mollapour, M., Bourboulia, D., Beebe, K., Woodford, M.R., Polier, S., Hoang, A., Chelluri, R., Li, Y., Guo, A., Lee, M.-J., 2014. Asymmetric Hsp90 N domain SUMOylation recruits Aha1 and ATP-competitive inhibitors. Molecular cell 53, 317-329.

Nath, S., Goodwin, J., Engelborghs, Y., Pountney, D.L., 2011. Raised calcium promotes alpha-synuclein aggregate formation. Mol Cell Neurosci 46, 516-526.

Nixon, R.A., Yang, D.-S., Lee, J.-H., 2008. Neurodegenerative lysosomal disorders: A continuum from development to late age. Autophagy 4, 590-599.

Pountney, D., Raftery, M., Chegini, F., Blumbergs, P., Gai, W., 2008. NSF, Unc-18-1, dynamin-1 and HSP90 are inclusion body components in neuronal intranuclear inclusion disease identified by anti-SUMO-1-immunocapture. Acta Neuropathologica 116, 603-614.

Pountney, D.L., Chegini, F., Shen, X., Blumbergs, P.C., Gai, W.P., 2005. SUMO-1 marks subdomains within glial cytoplasmic inclusions of multiple system atrophy. Neuroscience Letters 381, 74-79.

Radford, R., Wong, M.B., Pountney, D.L., 2014. Neurodegenerative aspects of multiple system atrophy. In: Kostrzewa, R.M. (Ed.), Handbook of Neurotoxicity 110. Springer Science + Business Media, New York (ISBN-13: 978-1461458357).

Rcom-H'cheo-Gauthier, A., Goodwin, J., Pountney, D.L., 2014. Interactions between calcium and alpha-synuclein in neurodegeneration. Biomolecules 4, 795-811.

Riedel, M., Goldbaum, O., Schwarz, L., Schmitt, S., Richter-Landsberg, C., 2010. 17-AAG Induces Cytoplasmic α-Synuclein Aggregate Clearance by Induction of Autophagy. PLOS ONE 5, e8753.

Sarge, K.D., Park-Sarge, O.-K., 2011. SUMO and its role in human diseases. Int Rev Cell Mol Biol 288, 167-183.

Schmid, A.W., Fauvet, B., Moniatte, M., Lashuel, H.A., 2013. Alpha-synuclein post-translational modifications as potential biomarkers for Parkinson's disease and other synucleinopathies. Molecular & cellular proteomics : MCP.

Silveirinha, V., Stephens, G.J., Cimarosti, H., 2013. Molecular targets underlying SUMO-mediated neuroprotection in brain ischemia. J Neurochem 127, 580-591.

Tanik, S.A., Schultheiss, C.E., Volpicelli-Daley, L.A., Brunden, K.R., Lee, V.M.Y., 2013. Lewy Body-like α-Synuclein Aggregates Resist Degradation and Impair Macroautophagy. Journal of Biological Chemistry 288, 15194-15210.

Tossidou, I., Himmelseher, E., Teng, B., Haller, H., Schiffer, M., 2014. SUMOylation determines turnover and localization of nephrin at the plasma membrane. Kidney international 86, 1161-1173.

Valera, E., Masliah, E., 2013. Immunotherapy for neurodegenerative diseases: focus on alpha-synucleinopathies. Pharmacology & therapeutics 138, 311-322.

Vijayakumaran, S., Wong, M.B., Antony, H., Pountney, D.L., 2015a. Direct and/or Indirect Roles for SUMO in Modulating Alpha-Synuclein Toxicity. Biomolecules 5, 1697-1716.

Vijayakumaran, S., Wong, M.B., Antony, H., Pountney, D.L., 2015b. Direct and/or indirect roles for SUMO in modulating alpha-synuclein toxicity. Biomolecules, Review ed.

Wang, X., Pattison, J.S., Su, H., 2013. Posttranslational Modification and Quality Control. Circulation Research 112, 367-381.

Weetman, J., Wong, M.B., Sharry, S., Rcom-H'cheo-Gauthier, A., Gai, W.P., Meedeniya, A., Pountney, D.L., 2013. Increased SUMO-1 expression in the unilateral rotenone-lesioned mouse model of Parkinson's disease. Neuroscience Letters 544, 119-124.

Wilkinson, K.A., Nakamura, Y., Henley, J.M., 2010. Targets and consequences of protein SUMOylation in neurons. Brain Res Rev 64, 195-212.

Winslow, A.R., Chen, C.-W., Corrochano, S., Acevedo-Arozena, A., Gordon, D.E., Peden, A.A., Lichtenberg, M., Menzies, F.M., Ravikumar, B., Imarisio, S., Brown, S., O'Kane, C.J.,

Rubinsztein, D.C., 2010. α-Synuclein impairs macroautophagy: implications for Parkinson's disease. The Journal of Cell Biology 190, 1023-1037.

Wong, M., Goodwin, J., Norazit, A., Meedeniya, A.B., Richter-Landsberg, C., Gai, W., Pountney, D., 2013. SUMO-1 is Associated with a Subset of Lysosomes in Glial Protein Aggregate Diseases. Neurotox Res 23, 1-21.

Xiong R, Zhou W, Siegel D, Kitson RR, Freed CR, Moody CJ, Ross D. 2015. A Novel Hsp90 Inhibitor Activates Compensatory Heat Shock Protein Responses and Autophagy and Alleviates Mutant A53T α-Synuclein Toxicity. Mol Pharmacol. 88, 1045-54.

Yang Y, Fiskus W, Yong B, Atadja P, Takahashi Y, Pandita TK, Wang HG, Bhalla KN. (2013) Acetylated hsp70 and KAP1-mediated Vps34 SUMOylation is required for autophagosome creation in autophagy. Proc Natl Acad Sci U S A. Apr 23;110(17):6841-6.

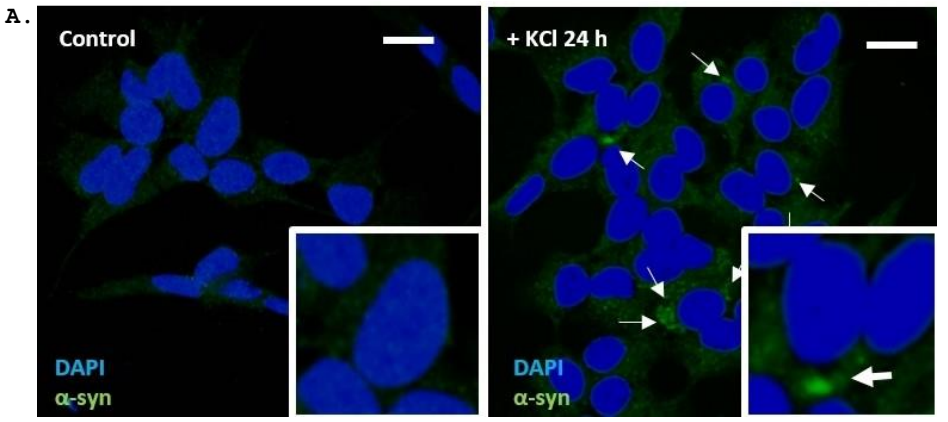
A.
Control
+ KCl 24 h
DAPI
α-syn
DAPI
α-syn

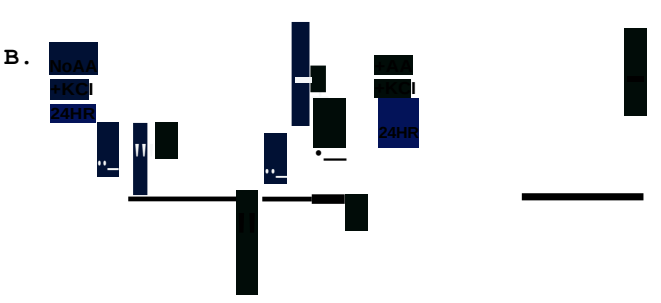
B.
No AA
+KCl
24HR
24HR

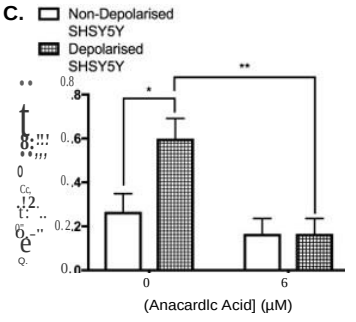
C.
Non-Depolarised SHSY5Y
Depolarised SHSY5Y
*
**
0.8
0.6
0.4
0.2
0.0
0
6
(Anacardlc Acid] (µM)

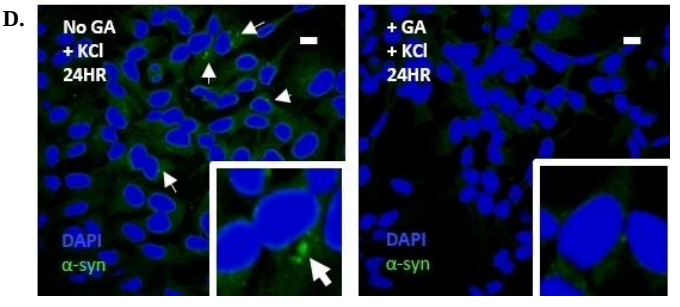
D.
No GA
+ KCl
24HR
+ GA
+ KCl
24HR
DAPI
α-syn
DAPI
α-syn

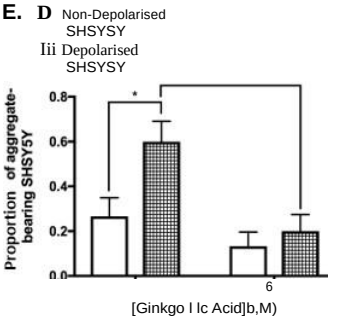
E.
D Non-Depolarised SHSYSY
Iii Depolarised SHSYSY
Proportion of aggregate-bearing SHSY5Y
0.8
0.6
0.4
0.2
0.0
*
6
[Ginkgo I lc Acid]b,M)

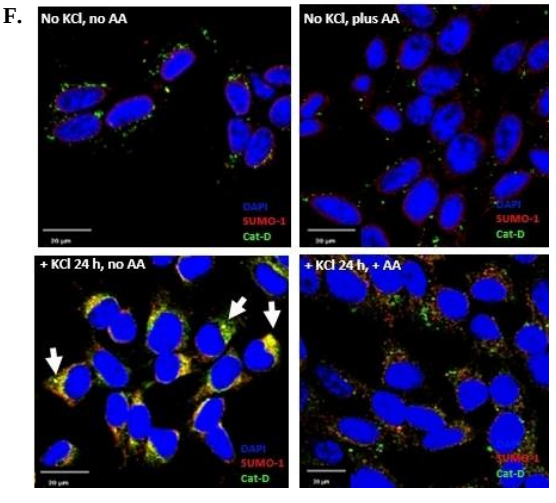
F.
No KCl, no AA
No KCl, plus AA
+ KCl 24 h, no AA
+ KCl 24 h, + AA
DAPI
SUMO-1
Cat-D

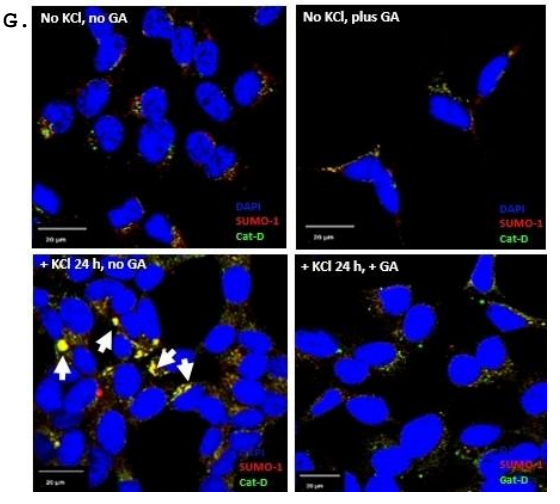
G.
No KCl, no GA
No KCl, plus GA
+ KCl 24 h, no GA
+ KCl 24 h, + GA
DAPI
SUMO-1
Cat-D

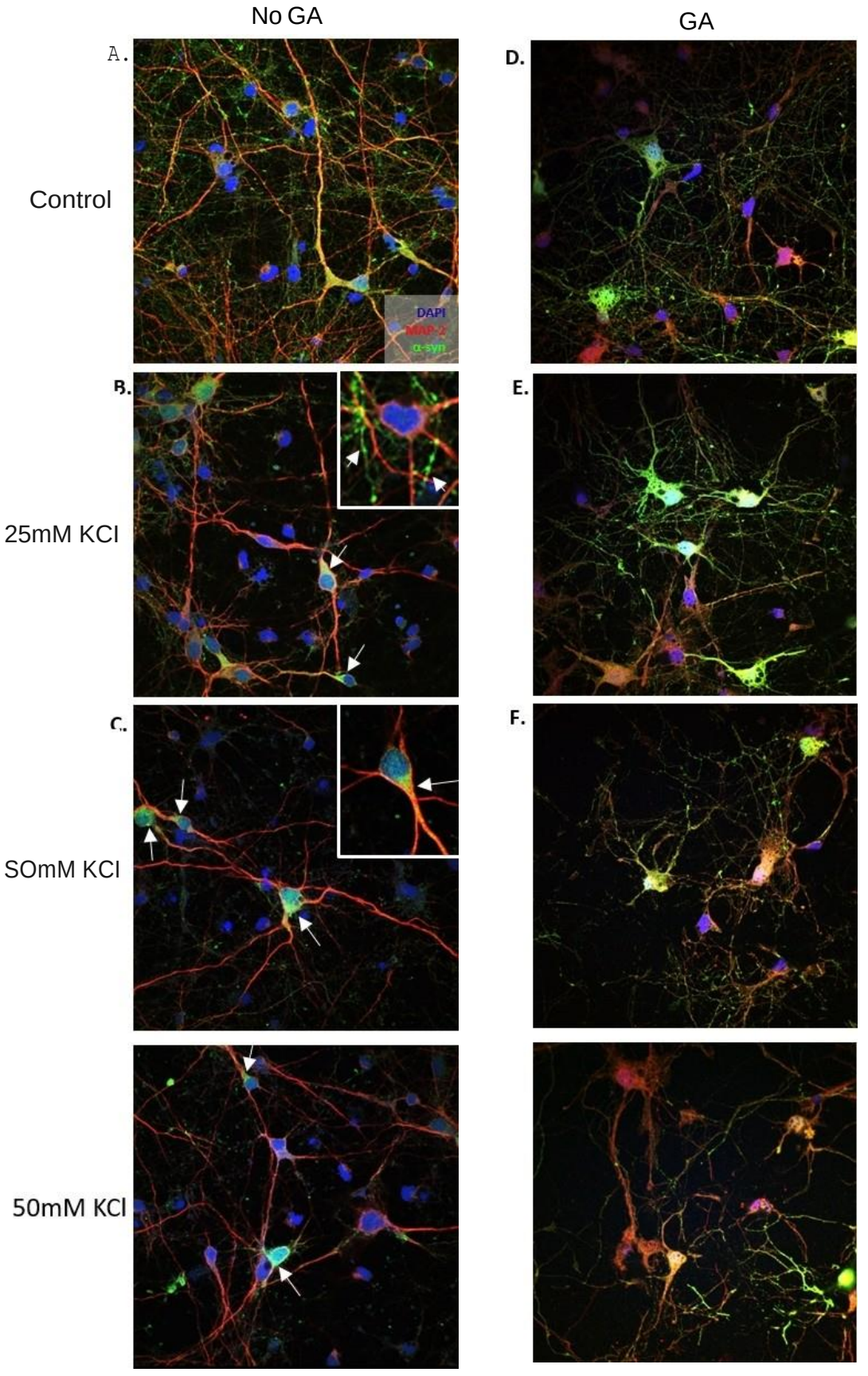
No GA
GA
A.
D.
Control
DAPI
MAP-2
α-syn
B.
E.
25mM KCl
C.
F.
SOmM KCl
50mM KCl

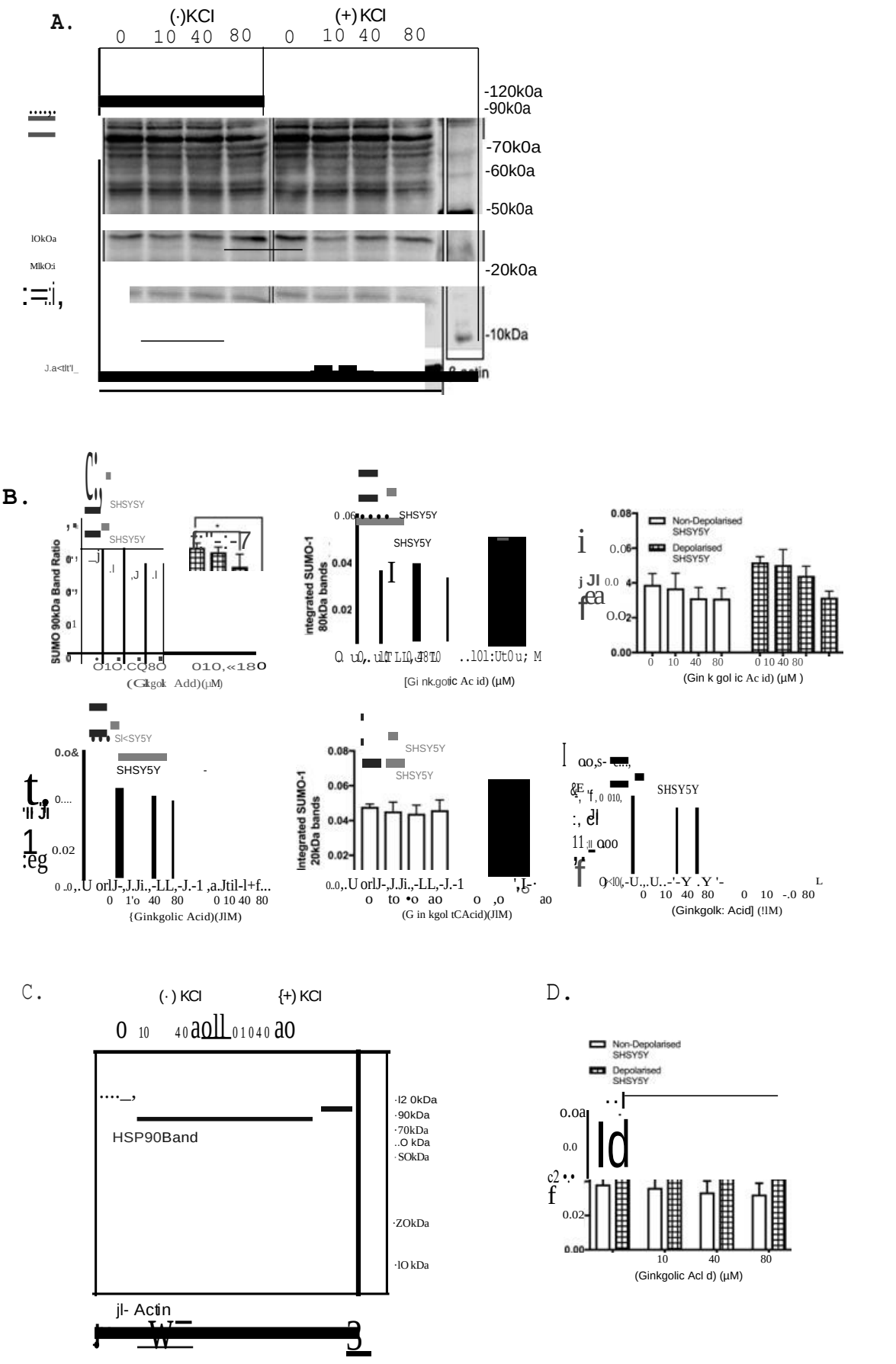
A.
(·)KCl
(+) KCl
0 10 40 80 0 10 40 80
-120k0a
-90k0a
-70k0a
-60k0a
-50k0a
-20k0a
-10kDa
lOkOa
MlkO:i
J.a<tlt'l_
B.
SHSY5Y
SHSY5Y
SUMO 90kDa Band Ratio
(Ginkgolk Add)(µM)
integrated SUMO-1 80kDa bands
[Ginkgolic Acid) (µM)
Non-Depolarised SHSY5Y
Depolarised SHSY5Y
(Ginkgolic Acid) (µM)
integrated SUMO-1 20kDa bands
{Ginkgolic Acid)(JlM)
(Ginkgolic Acid) (µM)
C.
(·) KCl
{+) KCl
HSP90Band
·l2 0kDa
·90kDa
·70kDa
·SOkDa
·ZOkDa
·lO kDa
jl- Actin
D.
Non-Depolarised SHSY5Y
Depolarised SHSY5Y
(Ginkgolic Acl d) (µM)

A.

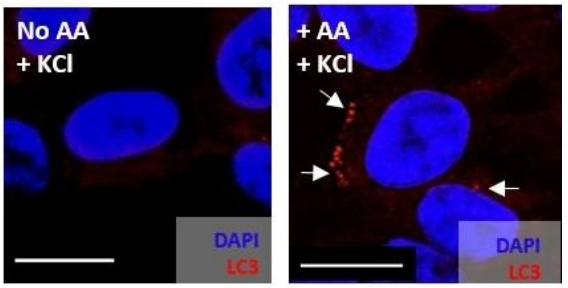

B. D Non-Oepolarisoo SHSYSY
El De polarised SHSY5Y

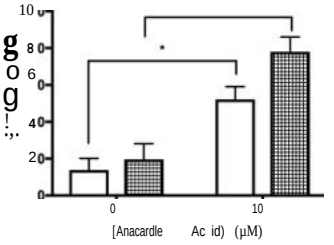

C.

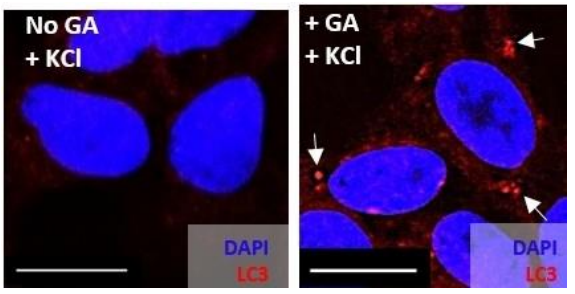

D. D Non-Depolarised SHSYSY
El Depolarised SHSYSY

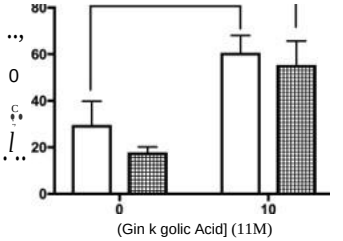

I. D Non-Depolarised SHSYSY
IIIII Depolarised SHSYSY

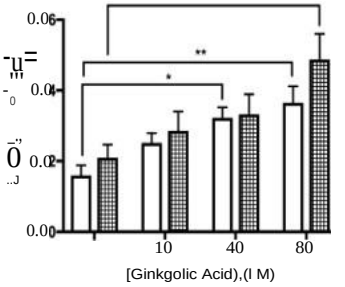

E.

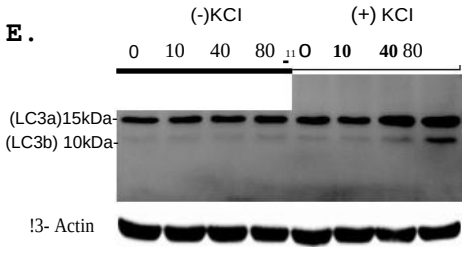

G.

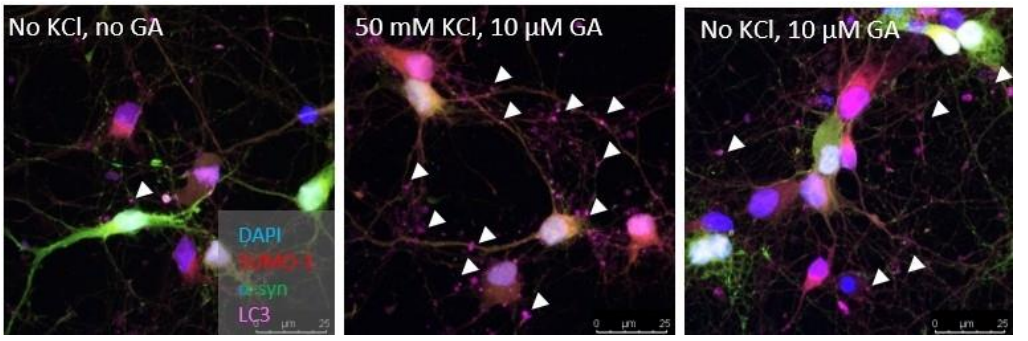

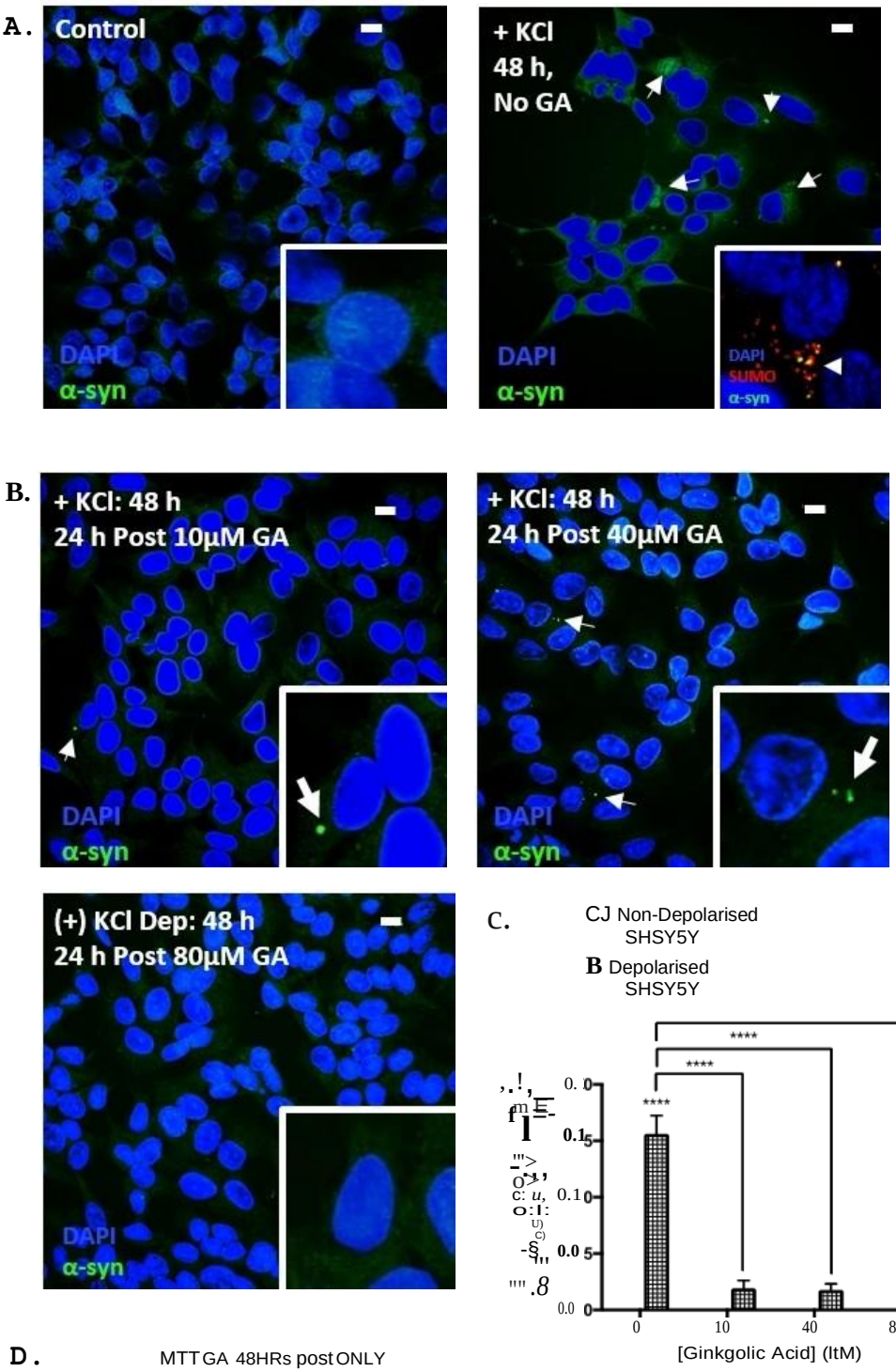
A.
Control
DAPI
α-syn
+ KCl
48 h,
No GA
DAPI
SUMO1
α-syn
B.
+ KCl: 48 h
24 h Post 10µM GA
DAPI
α-syn
+ KCl: 48 h
24 h Post 40µM GA
DAPI
α-syn
(+) KCl Dep: 48 h
24 h Post 80µM GA
DAPI
α-syn
C.
CJ Non-Depolarised SHSY5Y
B Depolarised SHSY5Y
****
****
****
0.0
0.1
0.0
0.0
0
10
40
80
[Ginkgolic Acid] (ltM)
D.
MTT GA 48HRs post ONLY
*
*
***
0.8
0.4
0.2
0.0
0
10
40
80
[Ginkgolic Acid) (1M)
Non-Depolarized SHSY5Y
Depolarised SHSY5Y

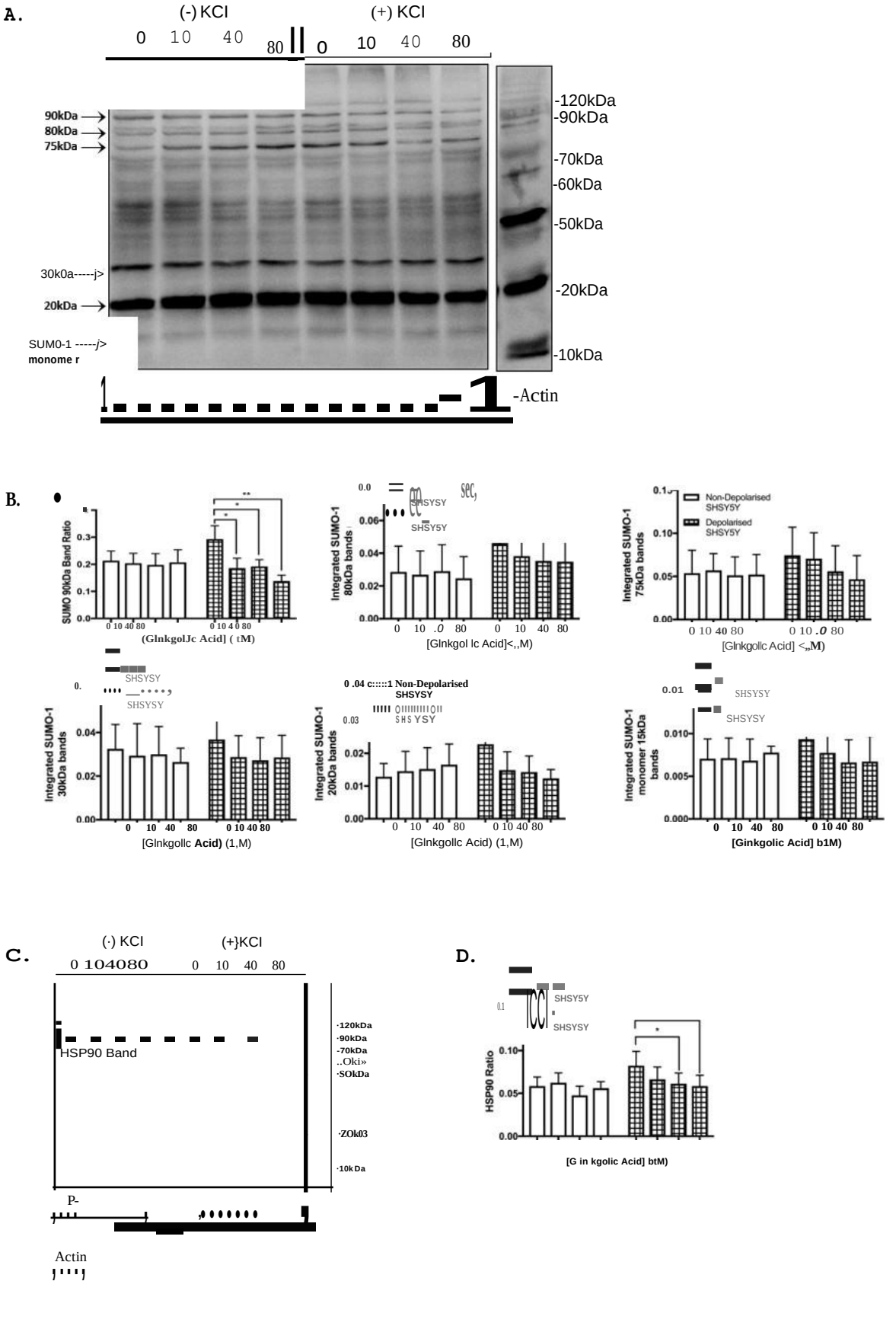
A.
(-) KCl
(+) KCl
0 10 40 80
0 10 40 80
90kDa
80kDa
75kDa
30k0a-----j>
20kDa
SUM0-1 -----j>
monome r
-120kDa
-90kDa
-70kDa
-60kDa
-50kDa
-20kDa
-10kDa
-Actin
B.
SUMO 90kDa Band Ratio
(GlnkgolJc Acid] (tM)
Integrated SUMO-1 80kDa bands
[Glnkgol lc Acid]<,,M)
Non-Depolarised SHSY5Y
Depolarised SHSY5Y
Integrated SUMO-1 75kDa bands
[Glnkgollc Acid] <„M)
SHSYSY
Integrated SUMO-1 30kDa bands
[Glnkgollc Acid) (1,M)
0 .04 c:::::1 Non-Depolarised SHSYSY
Integrated SUMO-1 20kDa bands
[Glnkgollc Acid) (1,M)
Integrated SUMO-1 monomer 15kDa bands
[Ginkgolic Acid] b1M)
C.
(·) KCl
(+}KCl
0 104080
0 10 40 80
HSP90 Band
·120kDa
·90kDa
-70kDa
..Oki»
·SOkDa
·ZOk03
·10kDa
P-
Actin
D.
SHSY5Y
SHSYSY
HSP90 Ratio
[G in kgolic Acid] btM)

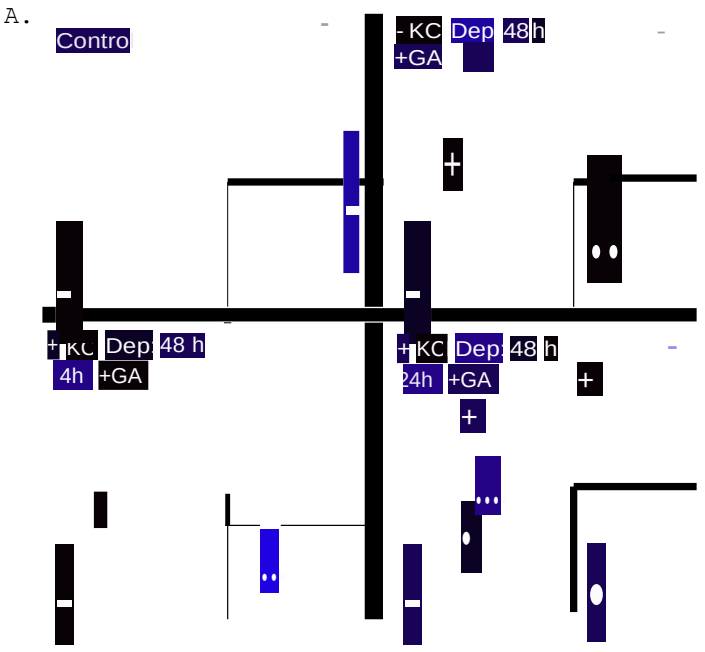
A.
Contro
- KC
+GA
Dep
48h
+KC
Dep
48 h
4h
+GA
+KC
Dep
48 h
24h
+GA

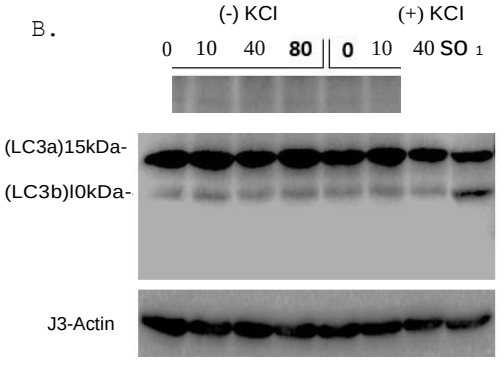
B.
(-) KCl
(+) KCl
0 10 40 80 0 10 40 SO
(LC3a)15kDa-
(LC3b)l0kDa-
J3-Actin

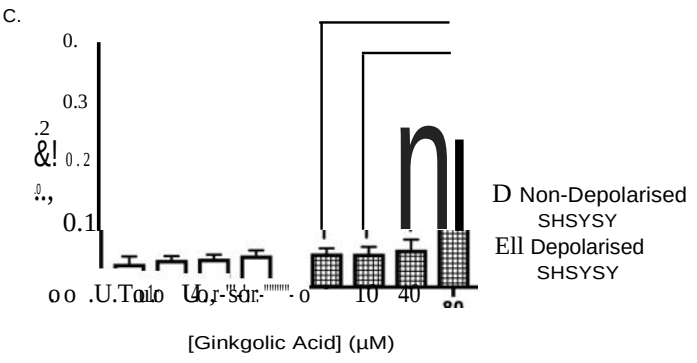
C.
0.
0.3
.2
0.2
0.1
D Non-Depolarised
SHSYSY
Ell Depolarised
SHSYSY
[Ginkgolic Acid] (µM)

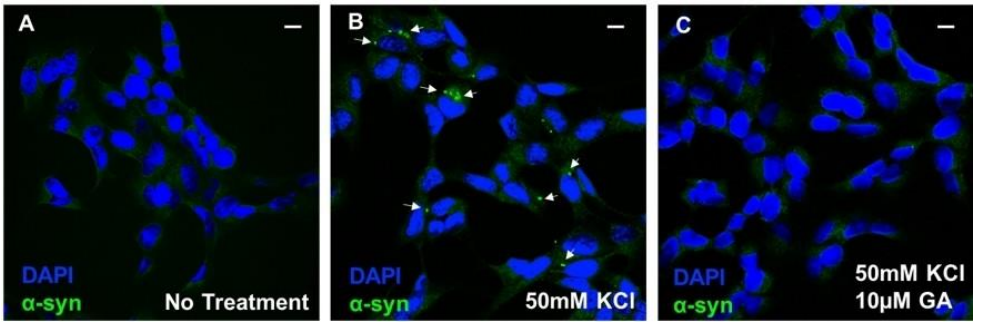
A
DAPI
α-syn
No Treatment
B
DAPI
α-syn
50mM KCl
C
DAPI
α-syn
50mM KCl
10μM GA

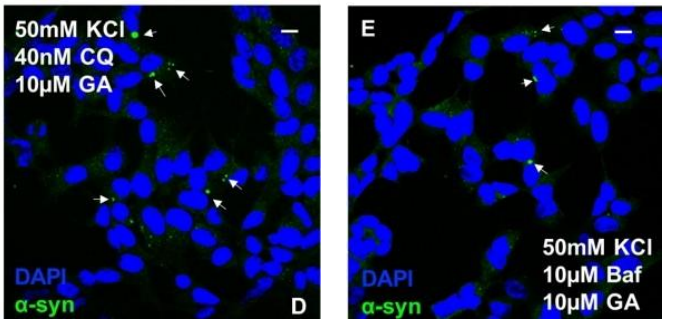
50mM KCl
40nM CQ
10μM GA
DAPI
α-syn
D
E
DAPI
α-syn
50mM KCl
10μM Baf
10μM GA

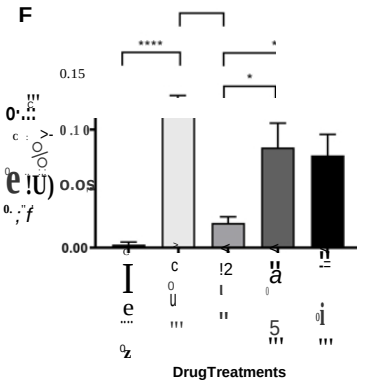
F
****
*
*
0.15
0.10
0.05
0.00
DrugTreatments
D No Treatment
D KCl Only
D KCVGA
• KCl/CQ/GA
• KCl/Baf/GA

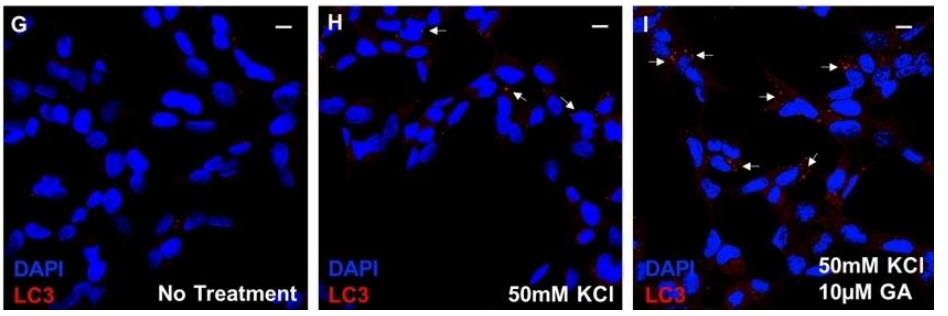
G
DAPI
LC3
No Treatment
H
DAPI
LC3
50mM KCl
I
DAPI
LC3
50mM KCl
10μM GA

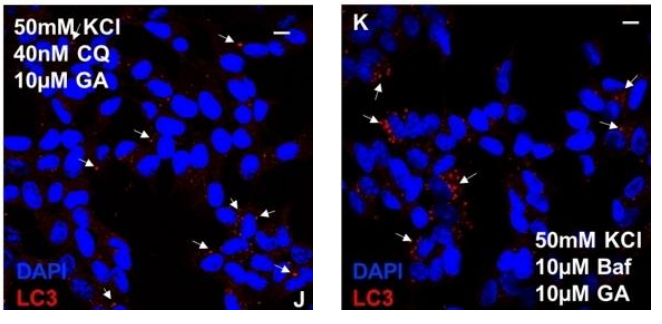
50mM KCl
40nM CQ
10μM GA
DAPI
LC3
J
K
DAPI
LC3
50mM KCl
10μM Baf
10μM GA

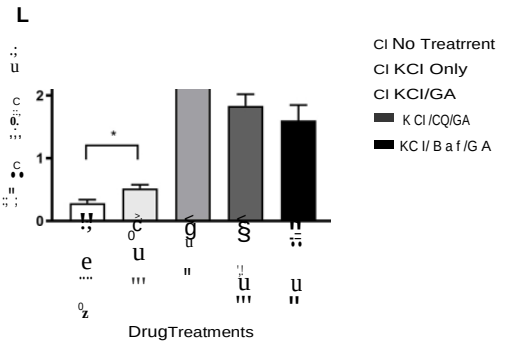
L
*
2
1
0
DrugTreatments
CI No Treatrrent
CI KCI Only
CI KCI/GA
K Cl /CQ/GA
KC l/ B a f /G A

A.

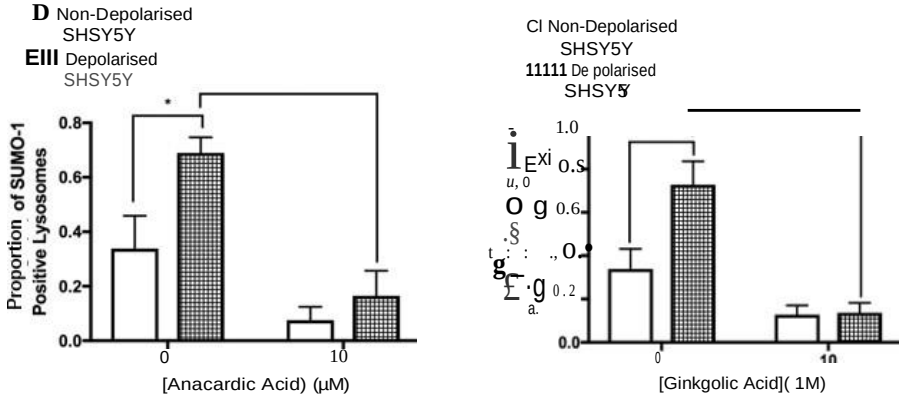
D Non-Depolarised SHSY5Y
EIII Depolarised SHSY5Y
Proportion of SUMO-1 Positive Lysosomes
0.0
0.2
0.4
0.6
0.8
0
10
[Anacardic Acid) (µM)
Cl Non-Depolarised SHSY5Y
11111 De polarised SHSY5Y
1.0
0.8
0.6
0.2
0.0
0
[Ginkgolic Acid](1M)

B.

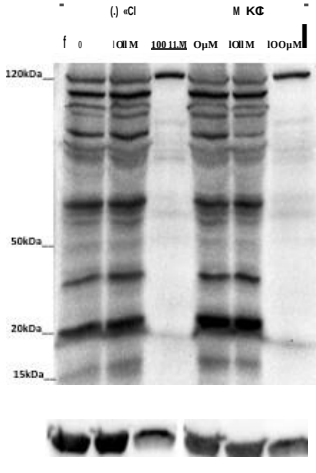
(-) «Cl
M KCl
f 0
100 11M
OµM
lOOµM
120kDa
50kDa
20kDa
15kDa

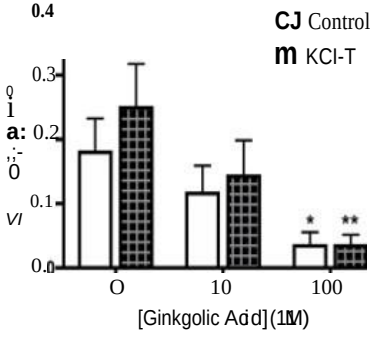
0.4
CJ Control
m KCl-T
0.3
0.2
0.1
0.0
O
10
100
[Ginkgolic Acid] (1M)